第 31 卷第 9 期
2015 年 9 月

无 机 化 学 学 报
CHINESE JOURNAL OF INORGANIC CHEMISTRY

Vol.31 No.9
1847-1854

一维和二维镝(Ⅲ)配合物的慢磁弛豫

吴建锋 张海霞 张 鹏 赵 朗 唐金魁*
(中国科学院长春应用化学研究所,稀土资源与利用国家重点实验室,长春 130022)

摘要: 分别用稀土醋酸盐和稀土高氯酸盐与希弗碱配体和巯基烟酸配体反应得到了两例镝配合物$[Dy_2(OAc)_6H_2O]_n$(**1**)和$\{[DyL(H_2O)_4]ClO_4\cdot H_2O\}_n$(**2**)(L=2,2′-二硫代-二(3-吡啶甲酸)),并通过单晶 X-射线衍射、元素分析、红外光谱和磁性测试对其进行了表征。结构研究和磁性测试表明:化合物 **1** 是羧基桥连的一维链结构,该化合物表现出慢磁弛豫性质,有效能垒为 2 K;化合物 **2** 是通过原位生成的二硫键桥连的二维网状结构,表现出明显的铁磁相互作用和慢磁弛豫行为。

关键词: 慢磁弛豫; 铁磁相互作用; 二硫键
中图分类号: O614.342 **文献标识码**: A **文章编号**: 1001-4861(2015)09-1847-08
DOI: 10.11862/CJIC.2015.236

Magnetic Relaxation in 1D and 2D Dysprosium(Ⅲ) Coordination Polymers

WU Jian-Feng ZHANG Hai-Xia ZHANG Peng ZHAO Lang TANG Jin-Kui*
(*State Key Laboratory of Rare Earth Resource Utilization, Changchun Institute of Applied Chemistry, Chinese Academy of Sciences, Changchun* 130022, *China*)

Abstract: Two dysprosium complexes, $[Dy_2(OAc)_6H_2O]_n$ (**1**) and $\{[DyL(H_2O)_4]ClO_4\cdot H_2O\}_n$ (**2**) (L=2,2′-dithiobis(3-pyridinecarboxylic acid)), were synthesized and structurally and magnetically characterized. Complex **1** is a 1D dysprosium chain, in which the dysprosium ions are bridged by OAc^- anions, exhibiting slow magnetic relaxation behavior with an energy barrier of 2 K. Complex **2** is a 2D dysprosium network, in which the carboxylato-bridged dysprosium chains are linked by disulfide bonds, showing ferromagnetic interaction and slow magnetic relaxation. CCDC: 1400117, **1**; 1400116, **2**.

Key words: slow magnetic relaxation; ferromagnetic interaction; disulphide bond

0 Introduction

Magnetic materials play an important role in our modern civilization and have driven great advances in the field of information technology, especially in high-density data storage [1-3]. However, the conventional magnetic materials are still limited by the superparamagnetic effect, preventing further increase of the storage density[4]. Since the discovery of single molecule magnet (SMM)[5-6], which exhibits magnetism at molecular level, the study of molecule based magnets has been the focus of chemistry, physics, and materials science[5]. In the past two decades, a major breakthrough have been procured in the study of single molecule magnet (SMM)[7-14] and single ion magnet (SIM)[13,15-19] both based on 3*d* metals, 4*f* metals [20-21], or both. Although single chain magnet (SCM)[22-25] is not dazzling enough to catch great attention among the research of molecule based magnets in contrast with SMM and SIM, it is promising to design and synthesize one dimensional[26-29], even two and three dimensional magnets, which behave magnetic relaxation. Herein,

收稿日期:2015-05-29。收修改稿日期:2015-07-13。
国家自然科学基金(No.21371166)资助项目。
*通讯联系人。E-mail:tang@ciac.ac.cn;会员登记号:S06N9843M1004。

we obtained two carboxylato-bridged dysprosium complexes, $[Dy_2(OAc)_6H_2O]_n$ (**1**) and $\{[DyL(H_2O)_4]ClO_4\cdot H_2O\}_n$ (**2**), with one and two dimensional structures. Magnetic study reveals that complex **1** shows slow magnetic relaxation behavior and complex **2** exhibits intra-chain ferromagnetic interaction and slow magnetic relaxation.

1 Experimental

1.1 Materials and general procedures

All chemicals and solvents were of analytical grade (Aladdin, Sigma-Aldrich) and used without any further purification. Elemental analysis for C, H, N and S wascarried out on a Perkin-Elmer 2400 analyzer. IR spectra (Fig.1) were recorded with a Perkin-Elmer Fourier transform infrared spectrophotometer using the reflectance technique (4 000~300 cm^{-1}) with samples prepared as KBr disks.

Caution! Perchlorate salts of metal complexes are potentially explosive. They should be handled with care and prepared only in small quantities.

1.2 X-ray crystal structure determination

Single-crystal X-ray data of the complexes were collected on a Bruker Apex Ⅱ CCD diffractometer

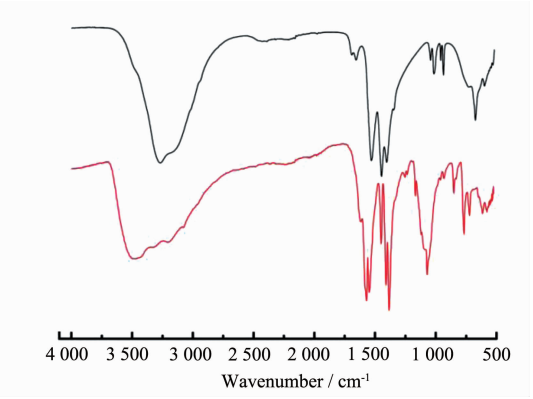

Fig.1 IR spectra of complexes **1** (black) and **2** (red)

equipped with graphite-monochromatized Mo-$K\alpha$ radiation (λ=0.071 073 nm) at 293(2) K. The structures were solved by direct methods and refined by full-matrix least-squares methods on F^2 using SHELXTL-97[30]. All non-hydrogen atoms were determined from the difference Fourier maps and refined anisotropically. The hydrogen atoms on the water molecules were determined from the difference Fourier maps. Other hydrogen atoms were introduced in calculated positions and refined with fixed geometry with respect to their carrier atoms. Crystallographic data are listed in Tables 1.

CCDC 1400117, **1**; 1400116, **2**.

Table 1 Crystallographic data for complexes 1 and 2

	1	**2**
Empirical formula	$C_{12}H_{20}Dy_2O_{13}$	$C_{12}H_{18}ClDyN_2O_{14}S_2$
Formula weight	697.38	676.35
Temperature / K	296(2)	296(2)
Crystal system	Monoclinic	Orthorhombic
Space group	*Ia*	*Cmca*
Z	4	8
a / nm	0.837 89(14)	2.363 57(11)
b / nm	1.653 5(3)	1.033 60(5)
c / nm	1.436 7(3)	1.947 28(10)
β / (°)	121.179(3)	121.013(2)
V / nm^3	1.981 1(6)	4.757 2(4)
Wavelength / nm	0.710 73	0.710 73
F(000)	1 312	2 648
D_c / ($g\cdot cm^{-3}$)	2.338	1.889
Completeness / %	99.7 (θ=25.17°)	100 (θ=25.1°)
Final *R* indices [$I>2\sigma(I)$]	0.018 0, 0.038 7	0.041 5, 0.119 7
R indices (all data)	0.018 6, 0.039 1	0.062 9, 0.137 8
Goodness of fit on F^2	0.922	1.096

1.3 Magnetic measurements

Magnetic susceptibility was recorded on a Quantum Design MPMS-XL7 SQUID magnetometer equipped with a 7 T magnet. The variable-temperature magnetization was measured in the temperature range of 1.9~300 K with an external magnetic field of 1 000 Oe. The dynamics of the magnetization were investigated from the ac susceptibility measurements with or without static fields and a 3.0 Oe ac oscillating field. Diamagnetic corrections were made with the Pascals constants[31] for all the constituent atoms as well as the contributions of the sample holder.

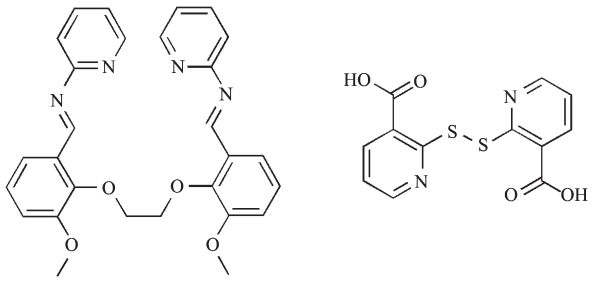

Scheme 1　Structural representations of ligand L_1 (left) and H_2L (right)

1.4 Synthesis of complexes 1 and 2

$[Dy_2(OAc)_6H_2O]_n$ (**1**). $Dy(OAc)_3\cdot 6H_2O$ (0.1 mmol) was dissolved in 10 mL CH_3CN/5 mL CH_2Cl_2, followed by the addition of L_1 (0.15 mmol). Then triethylamine (0.2 mmol, 28 μL) was added, and the mixture was stirred for 3 h. Colorless block-shaped single crystals, suitable for X-ray diffraction analysis, were isolated (70% yield based on $Dy(OAc)_3\cdot 6H_2O$) after 7 days. Elemental analysis Calcd. for $[Dy_2(OAc)_6H_2O]_n$ ($C_{12}H_{20}Dy_2O_{13}$, M_W=697.38): C, 20.67%; H, 2.89%. Found: C, 20.60%; H, 2.91%.

$\{[DyL(H_2O)_4]ClO_4\cdot H_2O\}_n$ (**2**). $Dy(ClO_4)_3\cdot 6H_2O$ (0.2 mmol) was dissolved in 8 mL CH_3OH/8 mL EtOH, followed by the addition of 2-thionicotinic acid (0.1 mmol). Then pyridine (0.1 mmol, 16 μL) was added, and the mixture was stirred for 5 h. Yellow block-shaped single crystals, suitable for X-ray diffraction analysis, were isolated (45% yield based on $Dy(ClO_4)_3\cdot 6H_2O$) after 4 days. Elemental analysis Calcd. for$\{[DyL(H_2O)_4]ClO_4\cdot H_2O\}_n$ ($C_{12}H_{18}ClDyN_2O_{14}S_2$, M_W=676.35): C, 21.31%; H, 2.68%; N, 4.14%; S, 9.48%. Found: C, 21.32%; H, 2.70%; N, 4.14%; S, 9.39%.

2 Results and discussion

2.1 Structure description of complex 1

The reactions of $Dy(OAc)_3\cdot 6H_2O$ with L_1 in the presence of triethylamine, afforded complex **1**. Details for the structure solution and refinement are summarized in Table 1, and selected bond distances and angles are listed in Table 2. Single-crystal X-ray (Fig.2) studies reveal that complexe **1** crystallizes in monoclinic space group *Ia* with Z=4. The structure can be described as one dimensional dysprosium chain linked by OAc^- without ligand L_1, suggesting a

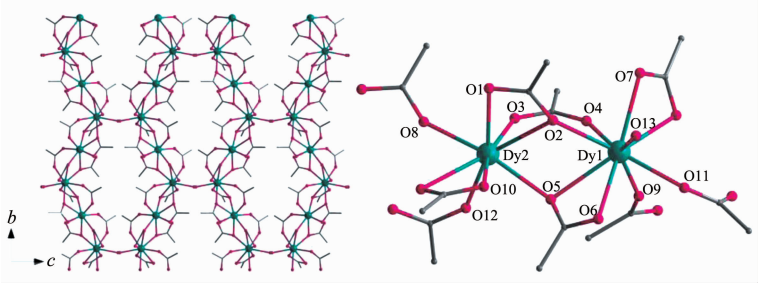

Hydrogen atoms have been omitted for clarity

Fig.2　1D chain structure (left) and coordination model (right) of **1** with azure, dark and red spheres representing Dy, C and O, respectively

Table 2 Selected bond distances (nm), angles (°) for complexes 1 and 2

Complex **1**			
Dy(1)-O(4)	0.233 0(5)	Dy(2)-O(9)	0.257 1(5)
Dy(1)-O(13)	0.235 8(4)	Dy(2)-O(12)	0.226 0(5)
Dy(1)-O(11)	0.234 4(5)	Dy(2)-O(3)	0.225 9(5)
Dy(1)-O(2)	0.238 2(5)	Dy(2)-O(8)	0.229 8(5)
Dy(1)-O(9)	0.238 9(5)	Dy(2)-O(10)	0.238 3(5)
Dy(1)-O(6)	0.242 9(5)	Dy(2)-O(5)	0.235 8(5)
Dy(1)-O(8)	0.245 1(5)	Dy(2)-O(1)	0.240 1(5)
Dy(1)-O(7)	0.248 3(5)	Dy(2)-O(2)	0.248 4(4)
Dy(1)-O(5)	0.255 4(5)	Dy(1)-Dy(2)	0.396 99(8)
Dy(1)-O(2)-Dy(2)	110.56(18)	Dy(2)-O(8)-Dy(1)	113.39(18)
Dy(2)-O(5)-Dy(1)	108.94(18)	Dy(1)-O(9)-Dy(2)	106.28(17)
Complex **2**			
Dy(1)-O(2)	0.229 4(5)	Dy(1)-O(3)	0.244 2(6)
Dy(1)-O(1)	0.230 2(5)	Dy(1)-O(4)	0.244 9(5)
Dy(1)-Dy(1)^{i}	0.516 80(6)		
O(1)-Dy(1)-O(3)	74.6(2)	O(1)-Dy(1)-O(4)	77.80(19)
O(2)-Dy(1)-O(3)	74.9(2)	O(1)-Dy(1)-O(3)	69.1(2)
O(2)-Dy(1)-O(4)	74.1(2)	O(2)-Dy(1)-O(1)	97.0(2)
O(3)-Dy(1)-O(4)	73.2(2)		

Symmetry cade: ^{i} 0.5−x, 1.5+y, z;

Table 3 Continuous Shape Measure (CShM) values calculated by SHAPE 2.1 for 1 and 2

Central atom	Coordination Geometry	Complex **1**	Complex **2**
Dy1	triangular cupola (C_{3v})	15.465	
	Capped cube (C_{4v})	10.868	
	Capped square antiprism (C_{4v})	1.703	
	Tricapped trigonal prism (D_{3h})	4.074	
	Hexagonal bipyramid (D_{6h})	12.385	16.67
Dy2/Dy1	Cube (O_h)	8.760	9.336
	Square antiprism (D_{4d})	4.424	2.816
	Triangular dodecahedron (D_{2d})	3.527	0.241

relative poor coordination ability of ligand L_1 (Scheme 1). The asymmetric unit is composed of two Dy^{III} ions, six OAc^- anions and one coordinated water molecule, in which the two Dy^{III} ions (Dy1 and Dy2) are linked by three OAc^- anions in two bridging modes: two of them are μ_2-η^1:η^2, the rest is μ_2-η^1:η^1 (Fig.2). The distance between Dy^{III} ions is 0.396 nm due to the μ_2-η^1:η^2 bridge. In such a distance, strong intramolecular magnetic coupling is not necessarily precluded. A closer look at the coordination sphere of Dy^{III} ions reveals that all the coordinating atoms are O atoms from OAc^- anions and water molecule. The introduction of water makes a great difference between the coordination spheres of Dy^{III} ions. Dy1 shows distorted mono-capped square-antiprismatic geometry as analyzed by the program SHAPE 2.1 (Table 3), with a water molecule as the cap atom, while, Dy2 shows triangular dodecahedral geometry in the

absence of coordinated water. Just because of the capped O atoms from water, the structure shows a zig-zag shape chain with Dy1 in the corner. Whats more, the corners of each chain are close to each other with the shortest inter-chain distance of 0.639 5 nm, which does not necessarily to preclude any inter-chain magnetic interactions.

2.2 Structure description of complex 2

The reactions of $Dy(ClO_4)_3 \cdot 6H_2O$ and H_2L with pyridine as the base afford complex **2**. In contrast with complex **1**, the structure of **2** (Fig.3), crystallized in orthorhombic space group *Cmca* with $Z=8$, is more complex and interesting. The asymmetric unit is composed of one Dy^{III} ion, one ligand L, one ClO_4^- and five water molecules, in which ligand L is derived from in-situ reaction of 2-thionicotinic acid. The structure can be described as two dimensional dysprosium network, in which one dimensional carboxyl bridged dysprosium chains are connected by ligand L. All Dy^{III} ions, in the same coordinating geometry, *i.e.*, four O atoms from ligands L and four coordinated water molecules construct triangular dodecahedral geometry, are linked by carboxyls from ligand L with common *syn-syn* bridging mode, forming one dimensional dysprosium chains. The dysprosium chains are linked by disulfide bonds, which are formed from *in-situ* reaction. The intra- and inter-chain distances are 0.517 nm and 0.974 nm, respectively.

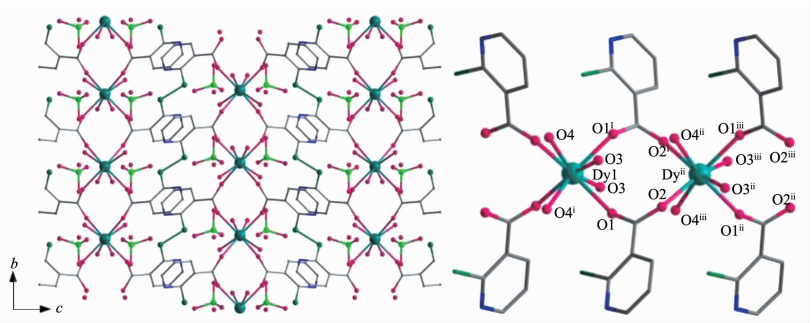

Hydrogen atoms and solvents have been omitted for clarity; Symmetry code: [i] 0.5−*x*, 1+*y*, 1.5−*z*; [ii] 0.5−*x*, 1.5+*y*, *z*; [iii] −1+*x*, 1.5+*y*, 1.5−*z*

Fig.3　2D network structure (left) and coordination model (right) of **2** with azure, dark, blue, green, cyan and red spheres representing Dy, C, N, Cl, S and O, respectively

2.3 Magnetic properties

The static magnetic susceptibilities of complexes **1** and **2** (Fig.4) were collected in the temperature range of 2~300 K under an applied magnetic field of 1000 Oe, and the magnetization (*M*) data were collected in the field range of 0~7 T below 5 K. The room temperature values of $\chi_M T$ (28.26 $cm^3 \cdot K \cdot mol^{-1}$ and 13.91 $cm^3 \cdot K \cdot mol^{-1}$, for **1** and **2**, respectively) are close to the expected value of 14.17 $cm^3 \cdot K \cdot mol^{-1}$ for each Dy^{III} ion, which indicates that the free-ion approximation applies. Upon cooling, however, the $\chi_M T$ values show different tendency, which is dependent on the magnetic interaction between Dy^{III} centers. For complex **1**, the $\chi_M T$ decreases slowly down to 10 K, reaching, after a sudden drop, the value of 17.23 $cm^3 \cdot K \cdot mol^{-1}$ at 2.0 K. The slow decrease and sudden drop are indicative of Stark level splitting at the lanthanide ions in weak crystal field and inter-chain or intra-chain antiferromagnetic magnetic interactions, respectively[32]. The field-dependent magnetization for **1** (Fig.5) rises abruptly at low fields and reaches $11.73\mu_B$ at 7 T without saturation, suggesting the presence of magnetic anisotropy[33]. In the case of complex **2**, the $\chi_M T$ decrease slowly down to 11 K and reaches a minimal value of 12.22 $cm^3 \cdot K \cdot mol^{-1}$, then increases suddenly and reaches the maximal value of 14.17 $cm^3 \cdot K \cdot mol^{-1}$ at 2.0 K. The inconstant $\chi_M T$ values suggest two possibilities: the presence of ferromagnetic coupling between Dy^{III} ions within the chain because the interchain magnetic interaction is relatively weak due to the long interchain Dy⋯Dy distance, or the occupation of Stark sublevels with higher $|J_z|$ values at low temperature[23]. The field-dependent magnetization for **2** (Fig.5) rises abruptly at

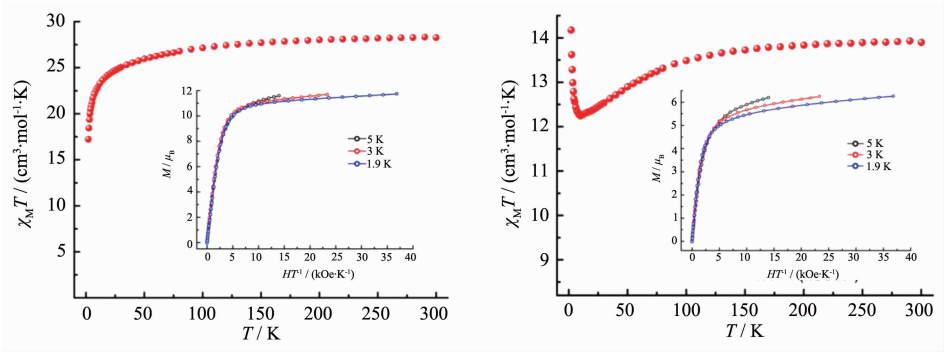

Fig.4 Temperature dependence of $\chi_M T$ products at 1 kOe, between **2** and 300 K for **1** (left) and **2** (right). Inset: plots of *M*-*H*/*T* for **1** and **2**

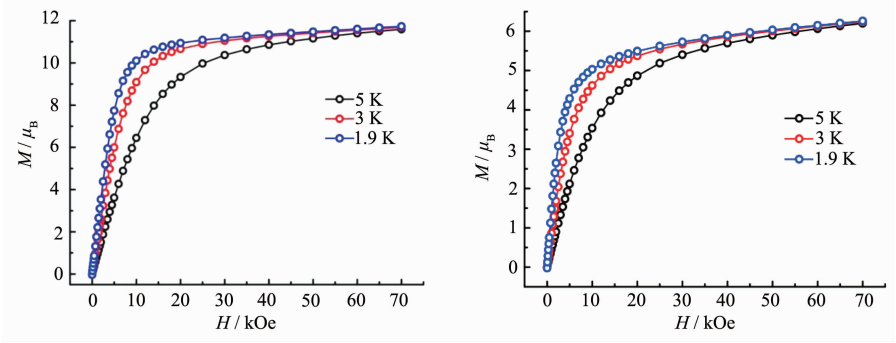

Fig.5 Field dependent magnetization for complexes **1** (left) and **2** (right) at 1.9, 3.0, and 5.0 K

low fields and reaches 6.26μ_B at 7 T without saturation, suggesting the presence of magnetic anisotropy or the considerable crystal-field effects[33].

In order to investigate the SMM behavior of **1** and **2**, alternating-current (ac) magnetic susceptibility measurements were also performed. Out-of-phase (χ'') susceptibilities signal aredetected for complexes **1** and **2** (Fig.6) under zero dc field, indicating slow magnetic relaxation behavior. Interestingly, the χ'' of complex **1** (Fig.7) under a 1 000 Oe dc field shows a small shoulder under 5 K. Upon cooling, the χ'' increases again at lower temperature region, indicating quantum tunneling process, which happens between the degenerated ground states[34-36]. The temperature-dependent ac susceptibility suggests the single-ion origin of such a slow relaxation behavior instead of single chain magnetism under 1 000 dc fields since the antiferromagnetic interaction detected in the static magnetic susceptibilities study is too weak to induce ordered magnetic moment arrangement. Although no maxima in χ'' are observed here, the energy barrier and τ_0 can be evaluated through the equation bellow[37-38]:

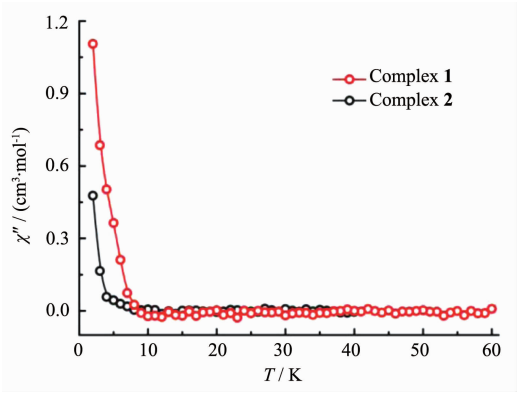

Fig.6 Temperature-dependent out-of-phase (χ'') susceptibilities for **1** and **2** at 1 000 Hz, under zero dc field

$$\ln(\chi''/\chi') = \ln(\omega\tau_0)+E_a/(k_BT) \quad (1)$$

The best fitting of $\ln(\chi''/\chi')$ vs. $1/T$ plots (Fig.9) gives an estimate of the activation energy and the characteristic time of ~2 K and 1×10^{-7} s, respectively.

Compared with **1**, χ'' for **2** below 5 K increase slower under zero dc field (Fig.6), indicating that the magnetic coupling between Dy^{III} ions is not strong enough to suppress the quantum tunneling effect. While, a new small shoulder appears at 7 K when 400

Oe dc field is applied (Fig.8), indicating slow relaxation of complex **2**. When lowering the temperature, χ'' increases rapidly, implying that quantum tunneling mechanism plays the dominant role in the low temperature region.

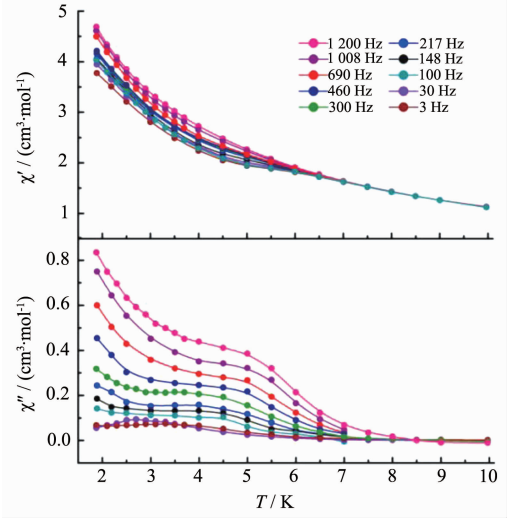

Fig.7　Temperature-dependent ac susceptibility for **1** under 1 000 Oe dc field

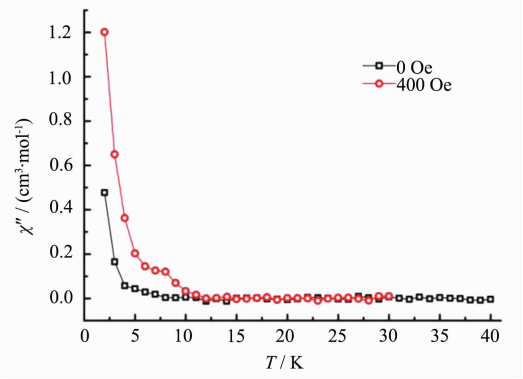

Fig.8　Temperature-dependent out-of-phase (χ'') susceptibilities for **2** at 1 000 Hz, under zero and 400 Oe dc field

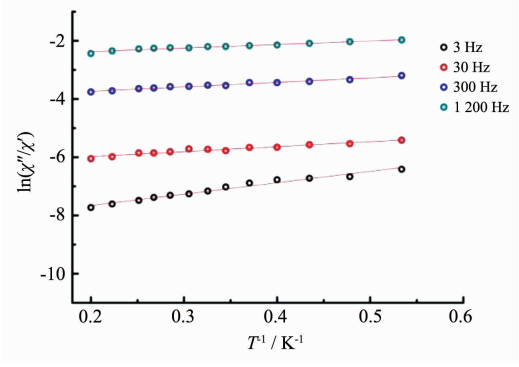

Solid line represents the fitting results over the range of 1.9~5 K

Fig.9　Plot of natural ln(χ''/χ') vs 1/T for **1**

3　Conclusions

In summary, 1D and 2D dysprosium complexes, **1** and **2**, have been isolated. Single crystal X-ray studies reveal that complex **1** is one dimensional zig-zag chain linked by OAc^- while complex **2** is two dimensional network constructed by disulfide bond bridged one dimensional dysprosium chains. Magnetic study shows that complex **1** exhibits slow magnetic relaxation behavior with energy barrier of 2 K, while complex **2** shows ferromagnetic magnetic interaction and slow magnetic relaxation.

References:

[1] Zhang P, Guo Y N, Tang J. *Coord. Chem. Rev*., **2013**,**257**:1728-1763

[2] Gatteschi D, Sessoli R, Villain J. *Molecular Nanomagnets*. Oxford: Oxford University Press, **2006**.

[3] Zhang P, Zhang L, Tang J. *Dalton Trans*., **2015**,**44**:3923-3929

[4] Stipe B C, Strand T C, Poon C C, et al. *Nat. Photonics*, **2010**,**4**:484-488

[5] Zhang P, Tang J. *Lanthanide Single Molecule Magnets*. Heidelberg: Springer, **2015**.

[6] LIN Shuang-Yan(林双燕), GUO Yun-Nan(郭云南), TANG Jin-Kui(唐金魁), et al. *Chinese J. Appl. Chem*.(应用化学), **2010**,**27**(12):1365-1371

[7] Blagg R J, Muryn C A, McInnes E J, et al. *Angew. Chem. Int. Ed*., **2011**,**50**:6530-6533

[8] Blagg R J, Ungur L, Tuna F, et al. *Nat. Chem*., **2013**,**5**:673-678

[9] Liu J L, Wu J Y, Chen Y C, et al. *Angew. Chem. Int. Ed*., **2014**,**53**:12966-12970

[10]Lin S Y, Wernsdorfer W, Ungur L, et al. *Angew. Chem. Int. Ed*., **2012**,**51**:12767-12771

[11]Tang J, Hewitt I, Madhu N T, et al. *Angew. Chem. Int. Ed*., **2006**,**45**:1729-1733

[12]Guo Y N, Xu G F, Wernsdorfer W, et al. *J. Am. Chem. Soc*., **2011**,**133**:11948-11951

[13]Zhang P, Zhang L, Wang C, et al. *J. Am. Chem. Soc*., **2014**, **136**:4484-4487

[14]Guo Y N, Ungur L, Granroth G E, et al. *Sci. Rep*., **2014**,**4**:5471

[15]Rinehart J D, Fang M, Evans W J, et al. *J. Am. Chem. Soc*., **2011**,**133**:14236-14239

[16]Joseph M Z, Dianne J X, Mihail Atanasov, et al. *Nat. Chem*.,

2013,**5**:577-581

[17]Rinehart J D, Fang M, Evans W J, et al. *Nat. Chem*., **2011**,**3**:538-542

[18]Ishikawa N, Sugita M, Ishikawa T, et al. *J. Am. Chem. Soc*., **2003**,**125**:8694-8695

[19]Ganivet C R, Ballesteros B, de la Torre G, et al. *Chem. Eur. J*., **2013**,**19**:1457-1465

[20]Woodruff D N, Winpenny R E P, Layfield R A. *Chem. Rev*., **2013**,**113**:5110-5148

[21]Dechambenoit P, Long J R. *Chem. Soc. Rev*., **2011**,**40**: 3249-3265

[22]Bogani L, Sangregorio C, Sessoli R, Gatteschi D. *Angew. Chem. Int. Ed*., **2005**,**44**:5817-5821

[23]Jia L, Chen Q, Meng Y S, et al. *Chem. Commun*., **2014**,**50**: 6052-6055

[24]Pejo C, Guedes G P, Novak M A, et al. *Chem. Eur. J*., **2015**,**21**:8696-8700

[25]Shao D, Zhang S L, Zhao X H, et al. *Chem. Commun*., **2015**, **51**:4360-4363

[26]Caneschi A, Gatteschi D, Lalioti N, et al. *Angew. Chem. Int. Ed*., **2001**,**40**:1760-1763

[27]Norio I, Yoshitomo O, Susumu C, et al. *J. Am. Chem. Soc*., **2008**,**130**:24-25

[28]Feng X, Harris T D, Long J R. *Chem. Sci*., **2011**,**2**:1688-1694

[29]Zhang Y Z, Zhao H H, Funck E, et al. *Angew. Chem. Int. Ed*., **2015**,**54**:5583-5587

[30]Sheldrick G M. *SHELXS*-97, *Program for Crystal Structure Solution*, University of Göttingen: Germany, **1997**.

[31]Boudreaux E A, Mulay L N. *Theory and Applications of Molecular Paramagnetism*. New York: John Wiley & Sons, **1976**.

[32]Kahn O. *Molecular Magnetism*. New York: VCH, **1993**.

[33]Xu G F, Wang Q L, Gamez P, et al. *Chem. Commun*., **2010**, **46**:1506-1508

[34]Leuenberger M N, Loss D. *Nature*, **2001**,**410**:789-793

[35]Plokhov D I, Popov A I, Zvezdin A K. *Phys. Rev. B*, **2011**, **84**:224436

[36]Wernsdorfer W, Sessoli R. *Science*, **1999**,**284**:133-135

[37]Bartolomé J, Filoti G, Kuncser V, et al. *Phys. Rev. B*, **2009**, **80**:014430

[38]Lin S Y, Xu G F, Zhao L, et al. *Dalton Trans*., **2011**,**40**: 8213-8217